Gas Sensing Properties of WO_3 Thick Film Resistors Prepared by Screen Printing Technique

ARUN S GARDE

Department of Physics, S P H A S C College Nampur (Nasik),
Savitribai Phule Pune University, Maharashtra, India.
E-Mail :arungarde@yahoo.co.in

Abstract

WO_3-based thick film resistors were fabricated using screen printing technology. The sensing behavior of WO_3 thick film resistors deposited on alumina substrates has been investigated for NH_3, H_2S, & LPG gas. The films were sintered at optimized temperature of 500^OC for 30 minutes. The material characterization was performed by XRD, SEM, and EDAX for elemental analysis. The UV-visible spectra show WO_3 exhibits a shoulder at 230 nm along with an ill-defined band at 251.6 nm. The optical band gap energy of 3.9 eV was obtained on a room temperature. The variation of D.C electrical resistance of WO_3 film samples was measured in air as well as in NH_3, H_2S, & LPG gas atmosphere as a function of temperature. The WO_3 film samples show negative temperature coefficient of résistance. The WO_3 film samples showed the highest sensitivity up to 400 ppm for NH_3 (2.94) at 300^OC, for H_2S (1.15) at 400^0C and for LPG (1.14) at 330^OC. Selectivity of H_2S and LPG gas in comparison with NH_3 was relatively poor. The effect of microstructure on sensitivity, response and recovery time of the sensor in the presence of NH_3, H_2S, & LPG gases were studied and discussed

Keywords: WO_3, Thick film, Material behavior, Optical behavior, Gas Sensitivity .

Introduction

Growing environmental pollution and a need to monitor and control these gases has led to research and development of very large variety of sensors using different materials and technology. In recent years, p and n-type semi conducting oxides have led to a new era in the field of gas sensors. Today our environment is polluted by number of gas exhausts from auto and chemical industries. Sensors play an important role in the areas of emissions control, environment protection, public safety, and human health [1-2]. Adverse and serious environmental issue has further promoted the development of sensors with both high sensitivity and rapid response. Metal oxide semiconductor materials such has SnO_2, ZnO, TiO_2, WO_3, Fe_2O_3, ZrO_2, CeO_2, In_2O_3, Cr_2O_3, $BaTiO_3$, Ga_2O_3 etc. have been well reported as gas sensors in the form of thick film [3]. The use of sensors is basically for industrial process controls, in human health, for the prevention of hazardous gas leaks, for measurements of physical quantities and for controlling some process leaks generated from manufacturing processes [4]. There are many types of gas sensors that have been used to detect various gases: catalytic gas sensors, infrared gas sensors, semiconductor gas sensors etc [1, 5-6]. Tungsten is the third element in group VI B of the Periodic Table. It Possesses different oxidation states ranging from (0) to (+VI) in various inorganic compounds. WO_3 has the oxidation state (+VI), its density is higher than Cr and Mo which are found in its group [6]. Tungsten oxide possesses a polycrystalline structure with a wide band gap semiconductor. The band gap energy in tungsten oxide is due to optical absorption which varies from 2.6-3.0 eV. The most common structure of WO_3 is monoclinic with space group $P2_1/n$.It is widely studied material owing to its established photochromic and electrochromic properties [7-8]. Amorphous and polycrystalline WO_3 films are

particularly attractive as gas sensors because they show a catalytic behavior both in oxidation and reduction reaction [9]. Electro chromic devices which exploit WO_3 are typically in an amorphous form, whereas electrical devices such as gas sensors are in a crystalline form [10]. Tungsten also forms other oxides such as WO, W_2O_3 and W_4O_3, however in gas sensing the stable WO_3 form is used. Tungsten Oxide is known to be a very promising material for sensing of the air pollutants like NO/NO_2, CO/CO_2 and ethanol [11-12].The sensing behaviour of bulk WO_3 is known to be a function of its chemical and physical properties such as surface area, phase composition, crystallinity, and stoichiometry. Generally, the majority of the WO_3 sensing properties are made up of (i) the WO_3 structural model perovskite- type ABO_3 lattice with A site being an unoccupied site, (ii) oxygen-deficient or non-stoichiometrical oxides and (iii) the sensitivity is being mainly influenced by the sensing material. The WO_3 based gas sensors are used because of their long term stability, small size, light weight, low cost, good mechanical strength, high reliability, fast response. WO_3 based gas sensors are synthesized in various forms such as Thin [13-15], Thick [16-21], Spray Pyrolysis [22]. The structural parameters like the crystallite size, Film thickness, and the porosity in the sensing layers have enhanced the effect on the gas sensitivity. The adsorption and desorption mechanism of semiconductor gas sensors is the simple mechanism of resistivity change. This resistivity change is due to the desorption of surface oxygen adsorbets via reactions with reducing gases such as H_2, CH_4, C_3H_8, C_2H_5OH, CO, LPG, NH_3 and H_2S.The reducing gas reacts with physisorbed oxygen, increasing the electronic concentration in the material thereby decreasing the electrical resistance [23]. As ammonia gas sensor is useful industrial product, it can be developed into gas sensors of low cost, high sensitivity and good selectivity. The resistance of all these n-type oxide semiconductor gas sensors is decreased by exposer to NH_3 gas. This is similar to the case of reducing gases. Liquefied Petroleum Gas (LPG) is highly inflammable gas, so it is explosively utilized in industrial and domestic fields as fuel. It is referred as cooking gas. Cooking gas consists chiefly of butane [24], a colorless, odorless and non toxic gas. Some well known materials for NH_3, H_2S and LPG gas sensing are ZnO [25-29], SnO_2 [30-33], Ru-SnO_2 [34], SnO_2-Cu [5, 35], TiO_2 [36-37], WO_3 [17, 38-40]. The aim of present work is to prepare WO_3 thick films by standard screen printing technique on alumina substrate and to investigate their sensing properties for NH_3, H_2S and LPG gas.

Experimental Details

Powder, Paste, Thick Film Preparation

Commercially available white color WO_3 powder (Loba Chem.) is mixed thoroughly in an acetone medium by using a mortar and pestle with a permanent binder (lead borosilicate glass frit with a composition of 70 wt.% PbO, 18 wt.% SiO_2, 3 wt.% Al_2O_3, 3 wt.% B_2O_3 and 6% TiO_2) [41]. Initially the fine powder is sintered at 450^oC for 2 hour in muffle furnace. The pastes used in screen- printing were prepared by maintaining inorganic to organic materials ratio at 70:30. The inorganic part consisted functional material (WO_3 and glass frit), the organic part consisted of 8% ethyl cellulose (EC) and 92% butyl carbitol acetate (BCA). A solution of EC +BCA (in ratio of 8:92) was made and added dropwise to the WO_3 powder until proper thixotropic properties of paste were achieved. The paste was screen printed onto an alumina substrate (96% pure Kyocera). The details of the technique are described elsewhere [42]. The films were dried under IR lamp for 1 hour in an air to remove the organic binder and fired at 500^OC for 30 minutes in the muffle furnace for better adhesion. During the firing process glass frit melts and the functional materials are sintered. The function of glass frit is to bind grains together.

Thickness Measurements

The thickness of the WO_3 thick films were measured by using Taylor-Hobson (Taly-step UK) system. The thickness of the films was observed in the range of 15-20 μm.

Material Characterizations

The WO_3 thick film material is characterized by X-ray diffraction technique [Miniflex model, Rigaku-Japan, DMAX-2500, CuKα (λ=1.542 angstrom) radiation] for structural analysis, degree of crystallinity and grain size determination for Braggs angle (2θ) from 20 to 80 degree. The average grain size was determined by using Debye Scherer formula [43]

$$D = \frac{0.9\lambda}{\beta \cos\theta} \qquad \text{.....(1)}$$

Where D is the grain size, λ is the wavelength of the X-ray radiation (1.542 angstrom), θ is the angle of diffraction and β is the full angular width of diffraction peak at the half maximum peak intensity.

Surface Morphology of the WO_3 thick films were studied by using scanning electron microscopy SEM (JOEL JED-2300, Japan) with Energy Dispersive Analysis of X-rays, EDAX for chemical composition. UV-VIS spectra were carried out on the JASCO UV-VIS-NIR Model V-670 Spectrophotometer.

Sensor Characterization

The DC resistance of the film samples was measured by half bridge method as a function of temperature in atmosphere [44]. The measurement of ppm-level gas sensing characteristics was carried out using a simple home built static measuring system [30] under normal laboratory conditions. The samples were characterized of NH_3, H_2S and LPG gas sensing for 400 ppm of gas concentration. The temperature of the sensor was increased from room temperature to 450^OC in air ambient. Before and after injecting the test gas (NH_3, H_2S and LPG), the change in the resistance of the sample was observed in air and test gas plus air. The optimal temperature of the sensor is defined as the temperature at which the sensor shows the maximum change in the resistance due to the presence of the test gas. The sensitivity (S_{ra}) of the WO_3 thick film sensors at various temperatures was calculated as

$$Sra = \frac{Rair}{Rgas} \qquad \text{..... (2)}$$

where R_{air} and R_{gas} are values of the resistance of the sensor in air and NH_3, H_2S and LPG gas plus air, respectively at the same temperature. The response time is defined as the time taken for the sensor to reach from 10% to 90% of the maximum value of the sensitivity after the surface has come in contact with the test gas [45]. The response time of the sensor was measured by injecting 400 ppm volume of gas inside the chamber at the optimal operating temperature of respective gas. For measuring recovery time, the sensor was exposed to air ambient by maintaining the optimal operating temperature constant, and then the time was noted till it achieved at least 10 % of its maximum value.

Result and Discussion

X-ray diffraction analysis of WO_3 thick film

Figure1. Shows an XRD patterns WO_3 thick film samples fired at 500^0C plotted in the range 20-80^0 (2θ). The XRD pattern shows several peaks of tungsten oxide phases indicating polycrystalline

nature. The observed peaks show the presence of different phases of WO_3, match well with reported ASTM data confirming polycrystalline structure. The sharp peaks reflexes seen on the pattern indicate that a transformation to a highly ordered crystallite has occurred in the material. As the firing temperature 500^0C, sharp and intense peaks appear in the XRD pattern indicating a high degree of crystallinity.

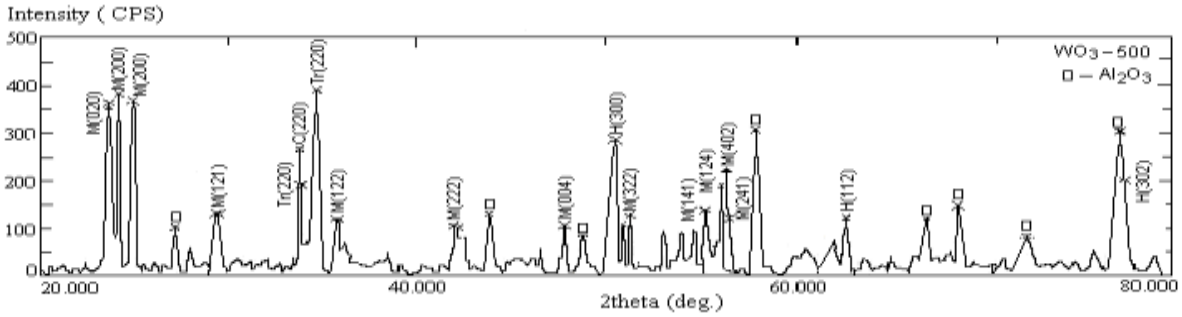

Figure1: XRD Pattern of WO_3 Thick film fired at 500^0C.

Firing Temp ^{0}C	% Relative phases of WO_3				
	WO_3 Monoclinic	WO_3 Triclinic	WO_3 Cubic	WO_3 hexagonal	Al_2O_3
500	50.79	10.70	5.24	11.67	21.60

Table1: The presence of % relative phases of WO_3 Thick film fired at 500^0C.

Table1. Illustrates the Presence of percentage relative Phases of WO_3 thick film resistor. Here I have added the intensities of all peaks corresponding to WO_3 and then the relative presence of different phases was found in percentage. It was also evident from fig.1. that the diffraction peaks at 2θ values of 23.7^0, 24.2^0, 24.9^0, 29.4^0, 42^0, 47.8^0, 50.9^0,51.3^0, 55.3^0, and 56.4^0 reveals the formation of the Monoclinic phase [ASTM Card No.43-1035], peaks at 33.9^0 and 34.7^0 reveals the formation of Triclinic phase[ASTM Card No.32-1395], peaks 50.5^0,62.8^0, and 77.6^0 reveals the formation of Hexagonal phase [ASTM Card No.33-1387] and Peak 33.8^0 reveal the formation of Cubic phase [ASTM Card No.46-1096]. In addition two reflections at 2θ=58, 77.3^0 corresponding to Al_2O_3 are also observed. The average grain size of the film samples calculated by using Scherer formula [43] were found to be 60.88 nm (±2nm) at 500^OC (±2 ^{O}C) respectively, which slightly higher than the earlier reported values (=55nm) [19].

Micro Structural Analysis by SEM

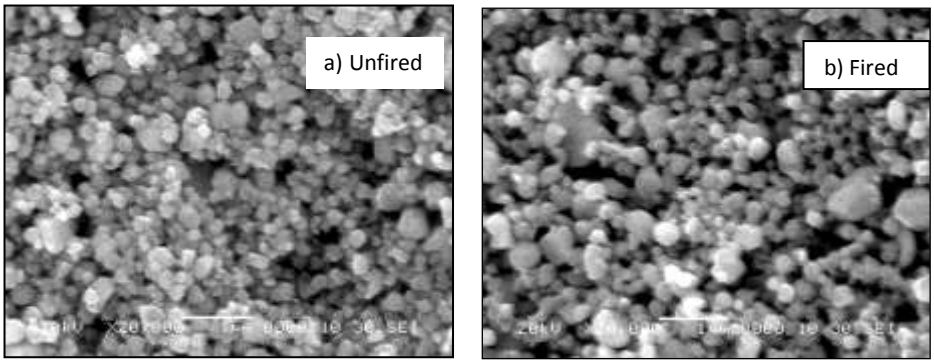

Figure 2: SEM image of WO_3 Thick film Fired at 500 ^{0}C. (a) Unfired WO_3 (b) Fired WO_3

Figure2-a and b shows the SEM micrographs of WO_3 thick films for studying the surface morphology. Figure 2 (a) shows the SEM micrograph of WO thick which were not fired at higher temperatures and I see the compactness in the polycrystalline structure without any pores. The Figure-2 b shows the SEM micrographs of WO_3 thick films fired at 500^{O}C. Here I see polycrystalline structure with number of pores (voids) distributed on the surface of the film, basically due to evaporation of organic binder during the firing of the films. The particle size is 325 nm (±2nm) at 500^{0}C (±2 ^{O}C) for the WO_3 thick film. The average particle size observed in SEM is much higher than estimated from bulk XRD data indicating agglomeration of the particles.

Elemental analysis

The EDAX analysis of WO_3 thick films showed presence of only W and O as expected, no other impurity elements were present in the WO_3 film samples. Also from the EDAX spectra, it is found that wt% and at% of W and O are nearly matched illustrate in Table 2.

Sample	Firing Temp ^{0}C	Wt %	Mass %	At %	Error %
WO_3	500	W	91.56	48.56	0.42
		O	8.44	51.44	0.41

Table2: Composition of the WO_3 Thick film fired at 500 ^{0}C

Optical studies

Figure 3- a Shows the absorbance spectra of WO_3 sample sintered at 450^{0}C in the wavelength range 200–800 nm.

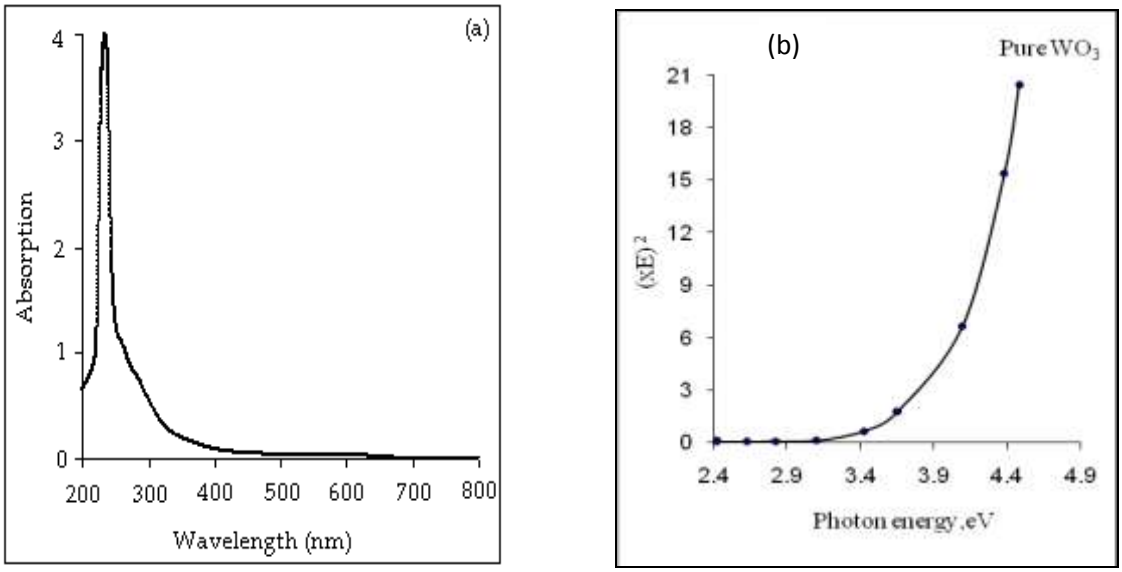

Figure 3: (a) Absorption spectra of WO_3 sintered at 450^{O}C (b) Plots of $(\alpha h\gamma)^2$ against $(h\nu)$ for WO_3.

The UV absorption spectra show the absorption peaks at around 251.6 nm. The data were further analysed for the estimation of the band gap energy of the WO_3 samples. The band gap of the WO_3 was

calculated by extrapolating the straight –line portion of the graph on X-axes plotted between $(\alpha h\nu)^2$ against the photon energy ($h\nu$) with the help of Tauc's relation-3 [46].

$$\alpha = \frac{A(h\gamma - Eg)^{1/2}}{h\gamma} \qquad \ldots\ldots (3)$$

Where *E*g is the optical band gap energy, *A* is a constant. Here n is equal to 1 for a direct gap. The obtained band gap from the graph was found to be 3.9 eV at room temperature shown in figure b. The optical band gap energy (E_g= 3.22 eV) of WO_3 has been reported by M.C.Rao [47].

Electrical characterization

The DC resistance of the WO_3 thick films fired at 500^0C ($\pm 2^0$C), was measured by using half bridge method as a function temperature. The resistance of thick films decreases with increase in temperature showing semi conducting behavior. Figure 4 a shows the resistance variation of WO_3 thick films fired at 500^0C (± 2 ^{0}C) temperatures in air. Tungsten oxide thick film samples exhibited three regions of resistance similarly to SnO_2 thick film Sensors [48]. There is a decrease in resistance with increase in temperature indicating semiconducting behavior, obeying $R=R_O\, e^{-\Delta E/KT}$ in the temperature range of 100 to 450^0C. For WO_3 film samples fired at 500^0C, initially resistance is constant up to 155^0C temperature, and then falls linearly up to a certain transition temperature. After the transition temperature the resistance decreases with exponential fashion and finally saturate to steady level. The transition temperature depends on firing temperature of the film. The resistance of WO_3 thick film samples upon exposer to NH_3, H_2S and LPG gas was lower than that in air. When gas comes in contact with grain boundaries there is systematic decrease in resistance of film upon exposer to NH_3, H_2S and LPG gas which is attributed to the decrease in potential barrier at grain boundaries. The initial value of WO_3 thick film resistance in air atmosphere (at 100^Oc) was measured to be 157885 Mohm.

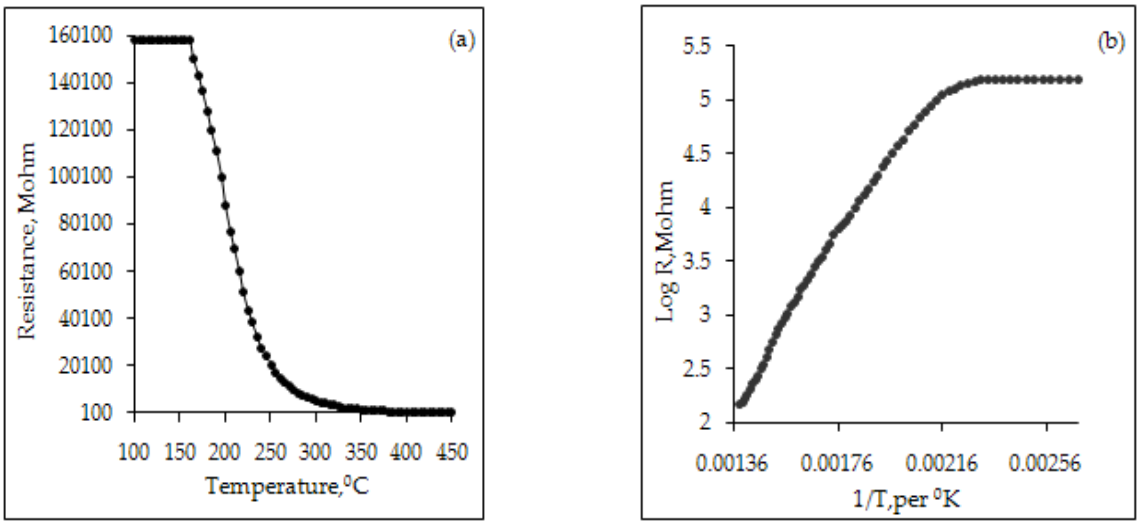

Figure 4: Variation of (a) Resistance with temperature (b) Log R Versus 1/T of WO_3 Thick film fired at 500^OC.

The following equation was used for calculating the resistance $R_{sample} = R_{ref}\,(V_{Supply}/V_{ref})$-1)]. Figure 4 b Shows log R versus reciprocal of temperature (1/T) variation of WO_3 thick films fired at

500^0C. This variation is reversible in both heating and cooling cycles obeying the Arrhenius equation

$$R = Roe^{-\Delta E / kT} \quad \ldots\ldots (4)$$

Where, Ro: the constant, ΔE: the activation energy of the electron transport in the conduction band, K: Boltzman constant and T: Absolute temperature.

It is seen that the curve has two distinct regions of temperature namely low temperature region (398 to 473^OK) and high temperature region (598 to 668^OK). The activation energy in the lower temperature region is always less than the energy in the higher temperature region because material passes from one conduction mechanism to another. The earlier reported value of activation energy is 0.82 eV [49]. In low temperature region, the increase in conductivity is due to the mobility of charge carriers which is dependent on the defect/dislocation concentration. So, the conduction mechanism is usually called the region of low temperature conduction. In this region activation energy decreases, because a small thermal energy is quite sufficient for the activation of the charge carriers to take part in conduction process. In other words the vacancies/ defects weakly attached in lattice can easily migrate (extrinsic migration). Hence increase in the conductivity in the lower temperature region can be attributed to the increase in charge mobility. In high temperature region, the activation energy is higher than that of low temperature region. In this region the electrical conductivity is mainly determined by the intrinsic defects and hence is called high temperature or intrinsic conduction. The high values of activation energy obtained for this region may be attributed to the fact that the energy needed to form defects much larger than the energy required for its drift. For this reason the intrinsic defects caused by the thermal fluctuations determine the electrical conductance of the film samples only at elevated temperature. The variation of resistivity, Temperature coefficient resistance (TCR) and activation energy of the WO_3 thick films fired at temperatures of 500^oC is summarized in Table 3.

Firing Temp. ^{0}C	Sheet resistivity $\rho_s x10^{12}$, (Ω/□)	TCR(/^{o}C) x 10^{-3}	Activation energy, eV	
			L.T. region	H.T region
500	0.09868	6.169	0.12582	0.86542

Table3: Electrical parameters of WO_3 Film samples fired at 500^OC. (Thickness =16 μm)

Sensing performance of Pure WO_3 Thick film

Figure 5, It is found that sensitivity of WO_3 thick films increases with increase in operating temperature and shows maximum peak values at optimal temperature and then the sensitivity decreases with further increase in temperature. At the optimal temperature, the activation energy may be enough to complete the chemical reaction. The resulting equation is

$$O_2\,(atm)+2e^-(cb) \rightarrow 2O^-_{ads} \quad \ldots\ldots\ldots(5)$$

The observed increase and decrease in the sensitivity indicates the adsorption and desorption phenomenon of the gases. The optimal temperature was confirmed for each WO_3 film samples for two cycles. For NH_3 gas, the response was observed to increase with operating temperature up to 300^OC. After $300\ ^0$C temperature, the surface would be unable to oxidize the gas so intensively and the NH_3 may burn before reaching the surface of the film at higher temperature. Thus, the gas sensitivity decreases with

increasing temperature [21]. The higher sensitivity may be attributed to the optimum number of misfits on the surface, porosity, larger surface area and the larger rate of oxidation of NH_3 at 300 ^{0}C for film. The maximum response of WO_3 thick film to NH_3 gas was found to be 2.944 at 300^{O}C. For H_2S gas, the response was observed to increase with operating temperature up to 400^{O}C and then decrease with a further increase in operating temperature. The maximum response of WO_3 thick film to H_2S gas was found to be 1.1567 at 400^{O}C. For LPG gas, the response was observed to increase with operating temperature up to 330^{O}C and then decrease with a further increase in operating temperature. The maximum response of WO_3 thick film to LPG gas was found to be 1.148 at 330^{O}C. The variation in the sensitivity with the temperature of the WO_3 sensor for 400 ppm of NH_3, H_2S, and LPG gas concentration in air is given in fig.5. Initially, the sensitivity increases with temperature and reaches a maximum values 2.944 at 300^{0}C for NH_3, 1.156 at 400^{0}C for H_2S and 1.148 at 330^{0}C for LPG. This temperature is known as the optimal temperature. The optimal temp reported for NH_3 with pure WO_3 thick film is 330^{0}C [16], for H_2S gas is in the range of 400 ^{0}C [21] and for LPG is reported as 325^{0}C [50]. The activation energy may be enough to complete the chemical reaction (eqn.5), which results in the maximum adsorption of the concerned gas and above the optimal temperature, the decrease in sensitivity with increase in the temperature, represents the rate of desorption of the reducing gas [R +O-ads =RO +e-]. The increase and decrease in the sensitivity observed in the graph represents the adsorption and desorption phenomenon of the gases. The change in resistance of the semiconductor oxide thick film sensor in the presence of toxic gases takes place according to the following two reactions [51]. In the first reaction, atmospheric O_2 molecules are physiosorbed on the surface site while moving from site and become ionized by taking an electron from the conduction band and are thus ionosorbed on the surface as O-ads [52]. This leads to an increase in resistance of the sensor material.

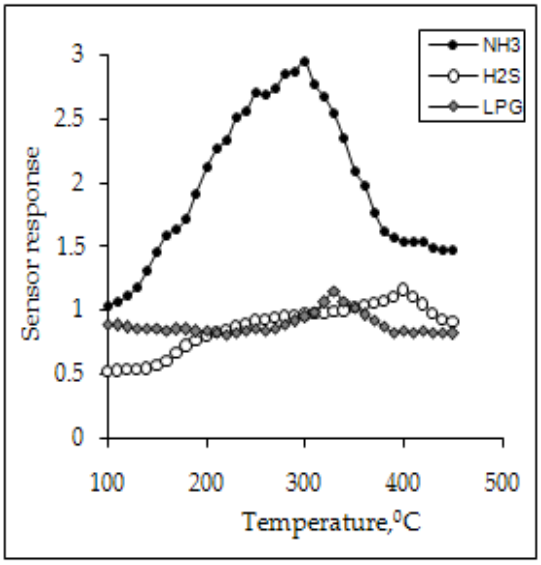

Figure 5: Sensor response with temperature of WO_3 Film for 400 ppm of NH_3, H_2S & LPG.

The resulting equation is O_2 (atm) + $2e^-$(cb) → $2O^-_{ads.}$ In the second reaction, the reducing gas (R), present in the ambient air, reacts with the chemisorbed oxygen, thereby releasing an electron back to the conduction band and decreasing the resistance of the sensor material R +O^-_{ads} =RO +e. Desorption of RO

takes place at a higher temperature. The basic reactions that might be taking place between the gas molecules and the surface –adsorbed oxygen species are as follows:

$O^-_{ads} + NH_3 \rightarrow NH + H_2O + e^-_{(cb)}$

$O^-_{ads} + H_2S \rightarrow S + H_2O + e^-_{(cb)}$

$13O^-_{(ads)} + C_4H_{10}\ (gas) \rightarrow 4\ CO_2\ (gas) + 5\ H_2O\ (gas) + 13e^-(cb)$

Response Time and Recovery Time

The time taken for sensor to attain 90% of maximum change in resistance or conductance upon exposure to NH_3, H_2S and LPG gas is the response time. The time taken by the sensors to get back 90% of original resistance or conductance is the recovery time. Figure 6.shows the typical change in response time for the WO_3 thick film sensors after injecting 400 ppm of test gas separately at the optimal temperatures 300^0C, 400^0C, and 330^0C for NH_3, H_2S and LPG gas into the measurement chamber. The response time is approximately 22 sec 10 sec and 10 sec. The recovery time is obtained just by removing the chamber. It was also found to be approximately 40sec, 50sec and 45sec. The quick response may be due to faster oxidation of gas.

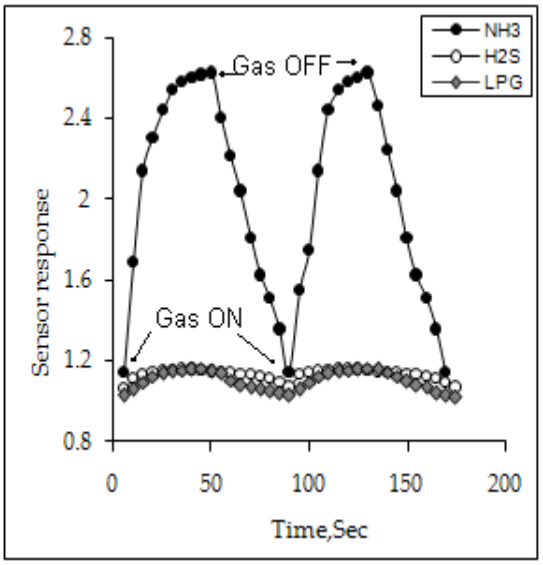

Figure 6: Sensor response with response time and recovery time of WO_3.

Selectivity for specific gas

Selectivity (or specificity) is a very important parameter for a gas to be useful. The operating temperature optimization studies can be used for the calculation of selectivity. The selectivity of gas for WO_3 thick film is calculated by using sensitivity data of fig.5. The selectivity of WO_3 thick film to 400 ppm is obtained for three gases NH_3, H_2S and LPG. The data for same are summarized in Table 4. From table it is seen that, at the operating temperature 300^0C, the selectivity for NH_3 against H_2S (3.0548) and LPG (3.1032), at the operating temperature 400^0C, the selectivity for H_2S against NH_3 (0.7493) and LPG (1.3796) and at the operating temperature 330^0C, the selectivity for LPG against NH_3 (0.4519) and H_2S (1.1611).The WO_3 film sample has good selectivity for NH_3 against H_2S and LPG. Selectivity of H_2S and LPG gas in comparison with NH_3 was relatively poor, as indicated by the adsorption configurations of the

gas molecules and fragmentation reaction on the W sites might be responsible for the high selectivity to NH_3.

Gas	Oper. Temp	Sensitivity	Selectivity			
NH_3	300	2.944	NH_3/ H_2S	3.054	NH_3/ LPG	3.103
H_2S	400	1.156	H_2S/ NH_3	0.749	H_2S/ LPG	1.379
LPG	330	1.148	LPG/ NH_3	0.451	LPG/ H_2S	1.161

Table 4: Selectivity data of WO_3 Thick film for NH_3, H_2S and LPG

Gas sensing mechanism

The gas sensing mechanism depends on the surface reaction between chemisorbed oxygen and reducing gases. The adsorption of oxygen on the film surface has two forms: physisorption and chemisorption. At elevated temperature, chemisorption is dominant. The transition from physisorption to chemisorption needs activation energy, which can be accomplished by increasing operating temperature. It has been reported that the amount of oxygen adsorbed on the sensor surface goes on increasing with an increase in temperature, reaches to maximum and then decreases with further increase in operating temperature. Ammonia acts as a reducing gas, the carrier concentration in the film rises as a result of the decrease in adsorbed surface oxygen. This rise in the electron concentration within the film is reflected as a decrease in resistance as follows [17].

$$2NH_3 + 3O^- \rightarrow N_2\downarrow + 3H_2O + 3e^-$$
$$4NH_3 + 5O_2 \rightarrow 4NO\downarrow + 6H_2O$$

H_2S is a reducing agent and reduces metal oxide to free metal.

$$WO_3 + 3H_2S \rightarrow W\downarrow + 3H_2O + S_3\uparrow$$

LPG gas on exposure decomposes into carbon and hydrogen species, which react with adsorbed oxygen, liberating the captured electrons into conduction band resulting in enhancing the catalytic activity of the film surface.

$$C_4H_{10}\ (gas) + 13O^-_{(film\ surface)} \rightarrow 4\ CO_2\ (gas) + 5\ H_2O\ (gas) + 13e^-(cb)$$

Conclusion

The screen-printed thick films of WO_3 on alumina substrate were used to detect the NH_3, H_2S and LPG gas at ppm level. XRD analysis shows the structure of WO_3 films is polycrystalline in nature. The average grain size of the WO_3 film samples were found to be 60.88 nm (±2nm) which is slightly higher than the earlier reported values. The average particle size observed in SEM is much higher than estimated from bulk XRD data, indicating agglomeration of the particles. From optical studies, the material involves direct transition with band gap energy value was found to 3.9 eV. The reported value of band gap of the WO_3 after heat treatment in air is attributed to the partial filling up of oxygen ion vacancies. The UV-visible spectrum of WO_3 exhibits a shoulder at 230 nm along with an ill-defined band at 251.6 nm. WO_3 thick films showed maximum response (2.944) to NH_3 at 300^OC, (1.156) to H_2S at 400^OC and (1.148) to LPG at 330^0C gas at optimal temperature. The gas response is very high to NH_3 as compared to H_2S and LPG. The quick response (~22 sec for NH_3, ~10 sec for H_2S and ~10 sec for LPG) may be due to faster oxidation of gas. Selectivity of H_2S and LPG gas in comparison with NH_3 was relatively poor, as

indicated by the adsorption configurations of the gas molecules and fragmentation reaction on the W sites might be responsible for the high selectivity to NH_3. From the above study I can see that WO_3 sensors have great effect and utility in industrial sector. Growing environmental pollution and a need to monitor and control these gases has led to research and development of very large variety of sensors using different materials and technology. So that WO_3 is best material for thick film gas sensors which possess high sensitivity and rapid response.

Acknowledgements

The author is grateful to Management authorities of M.G. Vidyamandir Panchavati Nasik for providing laboratory facilities for doing the work. Authors sincerely thank U.G.C. for financial assistance for this research project.

References

[1] A. Kolmakov, M.Moskovits, "Chemical Sensing and Catalysis by one Dimensional Metal Oxide Nanostructures", Ann.Rev.Mater.Res, 34, 151-180, 2004.

[2] Park Jinsoo, Shen Xiaoping, Wang Guoxiu, "Solvothermal synthesis and gas sensing performance of CO_3O_4 hollow nanospheres". Sensors & Actuators B, 136, 494-498, 2009.

[3] V. Guidi , M.A Uri Butt, M.C Carrotta, B. Cavicchi ,"Gas sensing Through Thick Film Technology", Sensors & Actuators B, 84,72-77, 2002.

[4] P.S. More, R.N. Karekar, S. Deshpande , N.D. Sali, S.V. Bhoraskar ,S. Sainkar, R.C. Aiyer , "Introduction of ∂-Al_2O_3/Cu_2O Material for H_2 gas Sensing Applications" Material Letters, 58 1020-1025, 2004.

[5] P.S.More, Y.B. Khollam, S. B. Deshpande, S. K. Date, R.N.Karekar, R.C. Aiyer, "Effect of variation of sintering temperature on the gas sensing characteristics of SnO_2-Cu (Cu=9wt%) system", Material Letters, 58, 205-201, 2003.

[6] M.A. Ouis , H.A.El-Batal, M.A. Azooz ,M.A. Abdelghany, "Characterization of WO_3- doped borophosphate glasses by optical, IR and ESR Spectroscopic Techniques before and after subjecting to gamma irradiation", Indian Journal of Pure & Applied Physics, Vol. 51-1,11-17, 2013.

[7] C.G.Granqvist in Handbook of Inorganic Electrochromic Materials. Elsevier Amsterdam, 1995.

[8] H.T. Sun C. Cantalini , L Lozzi , M. Passacantando, S. Santucci , "Micro structural effect on NO_2 sensitivity of WO_3 thin film gas sensors. Part I", Sensors and Actuators, 287,258-265, 1996. [9] H. H. Kung, Transition Metal Oxides: Surface Chemistry and Catalysis, Elsevier, NY, 1989.

[10] A. Takase, K. Miyakawa , "Raman study on sol-gel derived tungsten oxides form tungsten ethoxide", Jpn.J. Appl. Phys. 30 (8), 1508-1511, 1991.

[11] F. Ahmed, S. Nicoletti, S. Zampolli, Elmi, "Sensors and Microsystems in Proceedings of the 7th Italian Conference", Bologna, Italy 4-6 (2), 197-203, 2002.

[12] G. Sberveglieri, L. Depero, S. Groppelli, P. Nelli, "WO_3 sputtered thin films for NOx monitoring", Sensors & Actuators, B 26-27, 89-92,1995.

[13] Sobia Ashraf, Christopher S. Blackman, Robert G. Palgrave, Simon C. Naisbitt, Ivan P. Parkin, "Aerosol assisted Chemical Vapour Deposition of WO_3 thin films from tungsten hexacarbonyl and their gas sensing properties", Journal of Material Chemistry, 17, 3708-3713, 2007.

[14] L.G.Teoh , I.M.Hung, "High sensitivity semiconductor NO_2 Gas Sensor Based on Mesoporous WO_3. Thin film",Electrochemical and Solid State Letters, 6 (8), G108-G111, 2003.

[15] He Xiuli, Li Jianping , Gao Xiaoguang , "Effect of V_2O_5 coating on NO_2 sensing properties of WO_3 thin films", Sensors and Actuators B, 108, 207-210, 2005.

[16] Dong Hyun Yun, Chul Han Kwon, Hyung-ki Hong, Seung-Ryeol Kim, Kyuchung Lee, Ho Geun Song, Ji Eon kim, "Highly sensitive and Selective Ammonia Gas sensor", Transducers 1197 International conference on Solid state sensors and Actuators Chicago, June 16-19, 1997.

[17] Vibha Srivastava, Kiran Jain, "Effect of SiO_2 overlayer on WO_3 sensitivity to Ammonia", Sensors and Transducers Journal, 117 (6), 120-128, 2010.

[18] Jun Jae-Mok, Young-Ho Park, Chang-Seop Lee, "Characteristics of a Metal Loaded SnO_2/WO_3 Thick film Gas Sensor for Detecting Acetaldehyde Gas", Bull. Korean Chem.Soc., 32 (6) 1865-1872, 2011.

[19] M. Blo , M.C.Carotta, S. Galliera, S. Gherardi , A Giberti , V. Guidi ,C. Malagu , G. Martinelli , M. Sacerdoti , B. Vendemiati ,A. Zanni , "Synthesis of pure and loaded powders of WO_3 for NO_2 detection through thick film technology", Sensors and Actuators B, 103,213-218, 2004.

[20] R.S. Khadayate, R.B. Wghulde , M.G.Wankhede, J.V. Sali, P.P. Patil, "Ethanol vapour sensing properties of screen printed WO_3 thick films", Bull.Mater. Sci.30(2), 129-133, 2007.

[21] N.B.Sonawane, D.R. Patil , L.A. Patil , "CuO- Modified WO_3 Sensor for the Detection of a ppm Level H_2S gas at Room Temperature",Sensors and Transducers Journal, 93(6),82-91, 2008.

[22] M. Regragui, M. Addou , A. Outzourhit , J.C. Bernede , M.L. Idrisis , E. Benseddik, A. Kachouane ,Thin Solid films, 40,358-365, 2000.

[23] S. Shukla , S. Patil , S.C. Kuiry , Z. Rahman , T Du ,L. Ludwig ,C. Parish, S. Seal , Sensors & Actuators B, 96, 343-348, 2003.

[24] Z. Tianshu ,Z. Ruifang , S. Yusheng and L. Xingqin , "Influence of Sb/Fe ratio and heating temperature on microstructure and gas sensing property of Sb_2O_3-Fe_2O_3 complex oxide semiconductors", Sensors & Actuators B 32, 185-189, 1996.

[25] D.R. Patil, L.A. Patil , G.H.Jain , M.S. Wagh, S.A. Patil , "Surface Activated ZnO Thick Film Resistors for LPG Gas sensing", Sensors & Transducers Journal, 74(12), 874-883,2006.

[26] M.S.Wagh , G.H.Jain, D.R. Patil, S.A.Patil , L.A.Patil, "Modified Zinc oxide thick film resistors as NH_3 gas sensor", Sensors and Actuators, B 115, 128-133, 2006.

[27] V.R. Shinde , T.P. Gujar, C.D. Lokhande , R.S. Mane , "LPG sensing properties of ZnO films prepared by Spray Pyrolysis effect of molarity of precursor solution", Sensors & Actuators, B 120, 551-559, 2007.

[28] M. Aslam, V.A. Chaudhary, I.S. Mulla , S.R. Sainkar , A.B. Mandale, A.A. Belhekar, K. Vijayamohanan , "A highly selective ammonia gas sensor using surface ruthenated zinc oxide", Sensors & Actuators, 75, 162-167, 1999.

[29] G. Sarladevi , V.Balasubrahmanyam ,S.C. Gadkari, S.K. Gupta, "NH_3 gas sensing properties of nanocrystalline ZnO based thick films", Analytica Chimica Acta- xxx, 2006.

[30] Anil.D. Garje, Rohini C. Aiyer , "Effect of Firing Temperature on Electrical and Gas Sensing Properties of Nano-SnO_2-based Thick-Film Resistors", Int. J. Appl. Ceram. Tech.,4(5) 446-452, 2007.

[31] Kiran Jain, R. P. Pant, S. T. Lakshmikumar, "Effect of Ni doping on thick film SnO_2 gas sensor", Sensors & Actuators B, 113,823-829, 2006.

[32] L. Xingguing , C. Chunkua , X. Wendong , S. Yushenge, M. Guangyao, "Study on SnO_2-Fe_2O_3 gas sensing system by ac impedance technique", Sensors and Actuators B, 17, 1-5, 1993.

[33] A.S. Garde, "LPG and NH_3 Sensing Properties of SnO_2 Thick Film Resistors Prepared by Screen Printing Technique", Sensors & Transducers Journal, 122(11), 128-142, 2010.

[34] V.A. Chaudhari , I.S. Mulla, K. Vijayamohanan , "Impedance studies of an LPG sensor using surface ruthenated tin oxide", Sensors & Actuators B, 55, 127-133,1999.

[35] A.D.Inamdar, R.C. Aiyer, "High Performance SnO_2-Cu sensor for LPG and CO", Asian J. Phy. 9(1),1-8,2005.

[36] A.M.More , J.L. Gunjakar, C.D.Lokhande , "Liquified petroleum gas (LPG) sensor properties of interconnected web-like structured sprayed TiO_2 films", Sensors &Actuators B,129,671-677, 2008.

[37] D. Manno, G. Micocci , R. Rella , A.Serra, A.Taurino, A.Tepore, "TiO_2 thin films For NH_3 monitoring: structural and physical characterization", J. Appl. Phys.,82 (1), 54-59, 1997.

[38] Solis J.L, Sukko S., Kish L.B., Granqvist C.G., Lantto V.,"Nano-crystalline Tungsten Oxide Thick Films with High Sensitivity to H_2S at Room Temperature", Sensors &Actuators, B77 316-321, 2001.

[39] R. Ionescu , A. Hoel, C.G. Granqvist, E.Lolbet, P.Heszler,Sensors &Actuator B, 104,124-132, 2005.

[40] A. Masami , T. Takashi , S. Suto, S. Takahiro , N.Chiaki, M. Norio, N. Yamazoe , 'Ammonia gas sensor using thick film of an Au laoded tungsten trioxide' , Journal Ceramic Society Jpn.104 (12),1112-1116, 1996.

[41] L.I. Maissel , R. Glang (Eds.), Hand book of thin film technology. McGraw-Hill, New York, 1974.

[42] A.D.Garje, R. C. Aiyer, "Electrical and Gas-sensing Properties of a thick film resistor of nanosized SnO_2 with variable percentage of permanent binder", Int. J. Appl. Ceram.Technol, 3, 477-484, 2006.

[43] R.Y.Borse, A.S. Garde, "Effect of Firing temperature on electrical and structural characteristics of SnO_2 thick films", Indian J Physics, 82 (10), 1319-1328, 2008.

[44] G.Sarladevi, S. Manoramma, V.J.Rao, "Gas sensitivity of SnO_2/CuO heterocontact", J. Electrochemical society, 142 (8), 2574-2577, 1995.

[45] G.H. Jain, L.A. Patil , "Gas sensing properties of CuO and Cr activated BST thick films", Bulletin of Material Science, 29 (4), 403-411, 2004.

[46] C.H. Bhosale , A.V.Kamble, A.V. Kokate, K.Y.Rajpure ,"Structural, optical and electrical p properties of chemical sprayed CdO thin films", J.Materials Science &Engineering B,122 67-71, 2005.

[47] M.C.Rao and O.M.Hussain, "Optical Properties of Vacuum Evaporated WO_3 Films", Research Journal of Chemical Sciences, 1(7)10, 76-80, 2011.

[48] A. Chiorino ,G. Ghiotti , F. Prinetto , M.C. Carotta, C. Malagu, G. Martinelli , "Electrical and Spectroscopic characterization of SnO_2 and Pd-SnO_2 Thick films studied as CO Gas Sensors", Sensors & Actuators, B, 78, 89-95, 2001.

[49] A.Al.Mohammad, "Synthesis separation and electrical properties of WO_3-x Nano powders via partial pressure High Energy Ball-Milling", Acta Physica Poloncia, Vol.116, 241-244, 2009.

[50] L.A. Patil, J.P. Talegaonkar,"Synthesis of WO_3-polyaniline composites and their gas sensing properties", Sensors and Transducers Journal, 113 (2), 82-94, 2010.

[51] H. Windichmann, P. Mark, "A Model for the Operation of a Thin-Film SnO_x conductance-Modulation Carbon Monoxide Sensor", J. Electrochem. Soc.126, 627-633, 1979.

[52] J. Madaou, S. Morrison Roy, Chemical sensing with Solid State Devices Marc, Academic press, New York, 1989.